International Journal of Nanomedicine

Dovepress
Taylor & Francis Group

Open Access Full Text Article

ORIGINAL RESEARCH

Enhanced Antibacterial Effect of pH/Gelatinase-Responsive Florfenicol Nanogels Against *Staphylococcus aureus*

Nannan Leng[1,2,*], Jinhuan Liu[1,3,*], Yongtao Jiang[1], Ning Du[4], Ali Sobhy Dawood[5], Samah Attia Algharib[6], Wanhe Luo[1,2]

[1]College of Animal Science and Technology, Tarim University, Alar, Xinjiang, China; [2]Key Laboratory of Livestock and Forage Resources Utilization around Tarim, Ministry of Agriculture and Rural Areas, Tarim University, Alar, Xinjiang, China; [3]College of Veterinary Medicine, Sichuan Agricultural University, Chengdu, Sichuan, China; [4]Instrumental Analysis Center, Tarim University, Alar, Xinjiang, China; [5]Infectious Diseases Department, Faculty of Veterinary Medicine, University of Sadat City, Sadat city, Egypt; [6]Faculty of Veterinary Medicine, Benha University, Moshtohor, Egypt

*These authors contributed equally to this work

Correspondence: Wanhe Luo; Samah Attia Algharib, Email luowanhe0728@163.com; samah.alghareeb@fvtm.bu.edu.eg

Objective: *Staphylococcus aureus* (*S. aureus*) commonly endures in the body as small colony variations (SCVs), avoiding the bactericidal effects of drugs and leading to persistent and recurring mastitis infections in cows. Nevertheless, florfenicol is widely dispersed throughout the body and is challenging to penetrate to the targeted site at an appropriate therapeutic dosage, florfenicol's effectiveness in treating dairy cow mastitis caused by SCVs is comparatively low.

Methods: Florfenicol composite nanogels with sustained and targeted release effects were prepared by complexation of β-cyclodextrins (β-CD) and electrostatic interaction between gelatin (positive charge) and γ-polyglutamic acid (γ-PGA) (negative charge) using sodium tripolyphosphate (TPP) (ionic crosslinkers). The optimal formula of florfenicol composite nanogels was screened, and physicochemical characterization, in vitro release, and antibacterial activity of florfenicol composite nanogels were fully evaluated in this work.

Results: The optimal formulation was verified by producing florfenicol composite nanogels with 75 mg/mL β-CD, 150 mg/mL gelatin, 10 mg/mL γ-PGA, and 0.5 mg/mL TPP, respectively. The results of physicochemical characterization demonstrated that florfenicol composite nanogels were effectively generated by inclusion and electrostatic interaction. Furthermore, florfenicol composite nanogels exhibited obvious pH/gelatinase-double responsiveness. Furthermore, florfenicol composite nanogels were demonstrated a more potent bacteriostatic and bactericidal action against *S. aureus* and SCVs.

Conclusion: pH/gelatinase-double responsive florfenicol composite nanogels with sustained and targeted release effects can boost the antibacterial activity of florfenicol against SCVs.

Keywords: florfenicol, composite nanogels, small colony variants, sustained and targeted release, pH/gelatinase-double responsiveness

Introduction

Staphylococcus aureus (*S. aureus*) leads to a decrease in milk production and quality, an increase in treatment costs, and mortality rates of dairy cow's mastitis.[1] More seriously, *S. aureus* persists in the body in the form of *S. aureus* small colony variants (SCVs) due to long-term low-dose administration in animals.[2] When *S. aureus* changes from a normal state to SCVs, it will cleverly resist the host defense system and evade the bactericidal effect of antibiotics, thereby increasing bacterial resistance.[3] Veterinary antibacterial drugs are often used to treat bacterial diseases, such as dairy cow's mastitis caused by *S. aureus*. Among them, florfenicol's broad antibacterial spectrum, low dosage, low toxicity, acceptable safety, and notable therapeutic efficacy on bacterial infections in livestock and poultry caused by sensitive bacteria make it a popular choice for the clinical treatment of a variety of bacterial infectious disorders.[4–6] Due to its excellent antibacterial activity against *S. aureus*, it is speculated that florfenicol also has ideal antibacterial activity

Received: 30 December 2024
Accepted: 8 March 2025
Published: 23 April 2025

against SCVs. Nevertheless, florfenicol is widely dispersed throughout the body and is challenging to penetrate to the target site at an appropriate therapeutic dosage, florfenicol's effectiveness in treating dairy cow mastitis caused by SCVs is comparatively low.[7] Therefore, there is an urgent need to create a novel drug delivery system that has excellent sustained and targeted release effects in addition to ensuring the florfenicol's antibacterial effectiveness.

As a new drug delivery system, nanogels are a three-dimensional network system formed by various high molecular polymers and cross-linking.[8] In addition, nanogels with unique three-dimensional network structures can encapsulate antibacterial drugs and extend the action time of drugs in the body through sustained and targeted release effects to enhance their antibacterial activity.[9] The nanogels drug loading system can enhance the sustained release effect of florfenicol, thereby enhancing its antibacterial activity.[10] Similarly, the prepared florfenicol-chitosan nanocomposite also greatly improved the antibacterial activity against *Escherichia coli* ATCC 35218, *Salmonella Typhimurium* ATCC 14028, and *S. aureus* ATCC 29213 compared with the native drug.[11] In addition, florfenicol-loaded niosomes composed of Span 60, cholesterol, and dihexadecyl phosphate can improve antibacterial activity and bioavailability. This is because florfenicol-loaded niosomes exhibited a substantially higher maximum plasma concentration (C_{max}) and higher area under the curve (AUC_{0-t}) of florfenicol compared to free florfenicol.[12] Hydrogel material is very important for the preparation of nanogels. Among them, β-cyclodextrins (β-CD) have attracted a lot of interest from different drug carriers, because of their excellent interaction with hydrophobic guest molecules.[13] β-CD has been employed to improve the loading capacity of nanogels for poorly soluble pharmaceuticals and to encourage and maintain drug release. β-CD has an outer hydrophilic and inner hydrophobic structure, allowing it to accommodate most organic or inorganic molecules (such as florfenicol).[14] In addition, β-CD is both safe and non-toxic, soluble in water, and has a high loading capacity (LC) and encapsulation efficiency (EE). Therefore, it can improve the stability and solubility of drugs, reduce the toxic side effects of drugs themselves, enhance bioavailability and palatability, and is widely used in medicine and food.[15] However, the lack of targeted release properties of β-CD limits its clinical application in veterinary medicine. Interestingly, gelatin with gelatinase responsiveness can serve as a carrier for drug-controlled release systems, improving the bioavailability of drugs and achieving good targeted release properties.[16,17] Furthermore, γ-polyglutamic acid (γ-PGA) with pH responsiveness is an anionic polypeptide polymer with super water solubility, biodegradability, and biocompatibility, and can form a nanogel system by electrostatic assembly with other hydrogel material with positive charge (such as gelatin).[18]

In view of this, florfenicol may be encapsulated into β-CD to obtain florfenicol-β-CD inclusion complex (IC) through complexation, thereby improving the sustained release effect. Then, with the help of sodium tripolyphosphate (TPP) (ionic crosslinking agent), the γ-PGA-gelatin nanogels were prepared through the electrostatic interaction between gelatin (with positive charge) and γ-PGA (with negative charge), thereby improving the targeted release effect (the double responsiveness of gelatinase and pH). Furthermore, florfenicol composite nanogels with sustained and targeted release effects were prepared by complexation of β-CD and electrostatic interaction between gelatin (positive charge) and γ-PGA (negative charge) using TPP (ionic crosslinkers). Therefore, due to the sustained and targeted release effects of florfenicol composite nanogels, it is hypothesized that florfenicol composite nanogels can boost the antibacterial activity of florfenicol against SCVs (Figure 1). Thus, the creation and improvement of florfenicol composite nanogels was the main focus of this investigation. Several analytical techniques, including appearance, size, zeta potential (ZP), polydispersity index (PDI), transmission electron microscopy (TEM), scanning electron microscopy (SEM), energy-dispersive spectroscopy (EDS), X-ray diffraction (XRD), and Fourier transform infrared spectroscopy (FTIR), were used to determine the physicochemical parameters of the florfenicol composite nanogels. Moreover, the in vitro release and antibacterial activity of florfenicol composite nanogels were also fully evaluated.

Materials and Methods

Materials

β-CD, TPP, γ-PGA, and florfenicol were purchased from ChuangXin Pharmaceutical Co., Ltd. (China). Gelatin was purchased from Yongqinquan Intelligent Equipment Co., Ltd (China). Tryptone Soya Broth (TSB), phosphate-buffered saline (PBS), and physiological saline were obtained from Dingyuan Biotechnology Co., Ltd (China). A live/dead

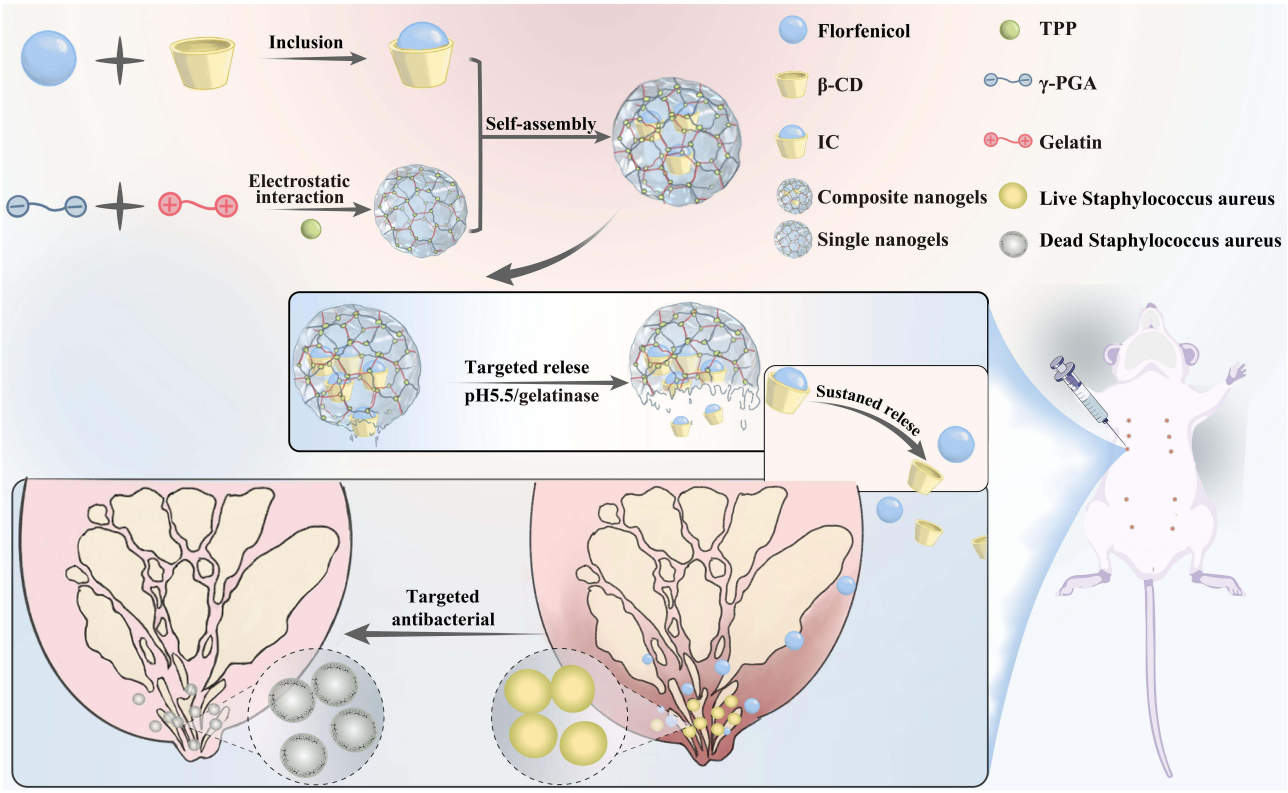

Figure 1 Schematic diagram of florfenicol composite nanogels with pH/gelatinase dual responsiveness for enhancing antibacterial activity against SCVs by sustained and targeted release effect.

backlight bacterial viability kit was offered by Shanghai Bestbio Biotechnology Co., Ltd. (China). The *S. aureus* 101 strain and SCVs 102 strain were provided by China Agricultural University (China) and characterized using the protocol reported elsewhere.[19]

Formulation of IC, Single Nanogels, Blank Nanogels and Florfenicol Composite Nanogels

A prior study's optimization and adaptation of the florfenicol-β-CD-IC was prepared.[20] In short, 10 mL ultrapure water was used to completely dissolve β-CD (0.025, 0.05, and 0.075 g) at a constant temperature of 80°C. To create the florfenicol-β-CD-IC, 200 mg of florfenicol was then added to the β-CD solution at 1000 RPM. Using TPP (ionic crosslinkers), the β-CD complexation and electrostatic interaction between the positively charged gelatin and negatively charged γ-PGA were used to create the florfenicol composite nanogels. Briefly, gelatin (0.5, 0.1, and 0.3 g) and γ-PGA (0.5, 0.1, and 0.3 g) were completely dissolved in 10 mL ultrapure water, respectively. Subsequently, 0.1 mL TPP (0.1, 0.2, and 0.3 mg/mL) was added into the γ-PGA and gelatin mixed solution by drops under the magnetic stirring at 1000 RPM. Finally, the florfenicol-β-CD-IC was added to the gelatin, γ-PGA, and TPP mixed solution to form florfenicol composite nanogels. Simultaneously, florfenicol single nanogels were prepared by florfenicol and electrostatic interaction between gelatin (positive charge) and γ-PGA (negative charge) using TPP (ionic crosslinkers). Blank nanogels were prepared by β-CD and electrostatic interaction between gelatin (positive charge) and γ-PGA (negative charge) using TPP (ionic crosslinkers).

Formula Screening

Standard Curve

Measure the OD values of different concentrations (25, 50, 100, 200, 500, and 1000 μg/mL) of florfenicol using a UV spectrophotometer (Lambda 365, PerkinElmer, USA) at an absorption wavelength of 266 nm, and plot the standard curves of florfenicol.

https://doi.org/10.2147/IJN.S511947

EE and LC

The prepared florfenicol composite nanogels were centrifuged at 14000 rpm for 60 min, the supernatant was taken and filtered, and the residual florfenicol in the supernatant was measured by ultraviolet spectrophotometer. The precipitated florfenicol composite nanogels were resuspended in ultrapure water. After the florfenicol composite nanogels were destroyed by the cell ultrasonic breaker, the supernatant was centrifuged at 8000 rpm for 10 minutes. The content of florfenicol in the filtered supernatant was determined by a UV spectrophotometer. EE and LC were calculated using the following formula:

EE = (content of florfenicol in nanogels/total amount of florfenicol) × 100%;
LC = (florfenicol content in nanogels/total amount of nanogels) × 100%.

Box-Behnken Response Surface Analysis

Furthermore, the Design-Expert 8.0 program (State-Ease, Inc., Minneapolis, MN, USA) provided precise results for the ideal concentrations of β-CD, gelatin, γ-PGA, and TPP. EE and LC were applied as assessment indices at the same time. Table 1 displays the Box-Behnken design's variables and levels.

Table 1 Single-Factor Experimental Design and Values of the Responses for Florfenicol Composite Nanogels

Run	β-CD (mg/mL)	Gelatin (mg/mL)	γ-PGA (mg/mL)	TPP (mg/mL)	LC (%)	EE (%)
1	25	150	30	1.5	12.6	36.8
2	75	150	30	1.5	7.8	33.1
3	25	50	30	0.5	18.4	39.4
4	25	50	10	1.5	7.9	29.8
5	75	150	10	0.5	21.8	45.6
6	50	100	30	1	16.3	38
7	50	100	20	1	11.8	39.5
8	75	50	30	0.5	17.9	44.7
9	50	100	20	1.5	15.7	38.3
10	75	50	30	1.5	15.2	39.6
11	50	100	20	1	11.8	39.5
12	25	150	10	1.5	21.9	42.5
13	75	50	10	1.5	12.5	33.2
14	50	100	10	1	18.4	38.6
15	25	50	10	0.5	8.5	30.5
16	50	150	20	1	15.7	38.6
17	75	50	10	0.5	14.4	41.1
18	25	50	30	1.5	14.3	39
19	50	100	20	0.5	17.4	39.3
20	50	100	20	1	11.8	39.5
21	75	100	20	1	8.4	39.6
22	50	100	20	1	11.8	39.5
23	50	100	20	1	11.8	39.5
24	75	150	10	1.5	22.8	43
25	25	150	10	0.5	21.4	38.6
26	25	150	30	0.5	14.7	32.5
27	75	150	30	0.5	12.6	36.3
28	50	50	20	1	12.5	36.9
29	25	100	20	1	7.2	36.4
30	50	100	20	1	11.8	39.5

Abbreviations: β-CD, β-cyclodextrins; γ-PGA, γ-polyglutamic acid; TPP, sodium tripolyphosphate; LC, loading capacity; EE, encapsulation efficiency.

Physicochemical Characterization

Surface Morphology

The appearance, TEM (JEM-2100Plus, JEOL, Japan), SEM (APREO, Thermo Scientific Inc., USA), and EDS (X-Max N 150, Oxford, UK) were utilized to characterize the surface morphology of florfenicol composite nanogels. Briefly, the freshly prepared florfenicol composite nanogels were placed in a bottle (0°, 45°, 90°, and 180°) to observe the gel state, respectively. Simultaneously, florfenicol composite nanogels were added to copper grids with thin slices, dried at room temperature with sodium phosphotungstate (2%) negative staining, and then the morphology was inspected by TEM. Subsequently, florfenicol composite nanogels were placed in a lyophilizer (FDU-1200, Huachen Instrument Co., Ltd, China) for freeze-drying to obtain lyophilized samples, and surface morphology of the lyophilized samples was observed by SEM at an accelerating voltage of 20 kV after oven drying. Furthermore, elemental analysis of the freeze-dried florfenicol composite nanogels was determined by EDS.

The Mean Size and ZP

The mean size and ZP of IC, single nanogels, blank nanogels, and florfenicol composite nanogels were measured using Zetasizer ZX3600 "Malvern Instruments, Malvern Instruments Limited, UK".

XRD and FTIR

XRD and FTIR spectrophotometer of β-CD, gelatin, γ-PGA, TPP, lyophilized IC, single nanogels, blank nanogels and florfenicol composite nanogels were analyzed using an X-ray diffractometer "Bruker D8 Advance, BRUKER OPTICS, Germany" and an FTIR spectrophotometer "Nicolet iS50, Thermo Scientific Inc., USA".

In vitro Responsive Release

Since the freeze-dried IC is in powder form and cannot form lumps, the in vitro release of IC has not been measured. Thus, lyophilized single nanogels, blank nanogels, and florfenicol composite nanogels were immersed in 10 mL PBS (pH 5.5/7.4) with or without gelatinase at 37°C in this study. At 0, 0.5, 1, 2, 3, 4, 6, 8, 12, and 24 h, the changes in the morphology of lyophilized single nanogels, blank nanogels, and florfenicol composite nanogels in PBS (pH 5.5/7.4) with or without gelatinase were observed. Subsequently, florfenicol composite nanogels were diluted with PBS and then put into a dialysis bag (MW: 3500). The dialysis bags containing the florfenicol composite nanogels (100 mg/mL) were placed into 500 mL PBS (pH 5.5/7.4) without and with gelatinase at 37±0.5°C. At different time points (0.5, 1, 2, 4, 8, 12, and 24 h), 1 mL dialysate was taken out and blank PBS with equal temperature (37±0.5°C) and volume (1 mL) was added. Subsequently, the florfenicol concentrations were determined by UV spectrophotometer. Ultimately, the cumulative release % was used to design the in vitro release curves of florfenicol composite nanogels in various microenvironments (pH 5.5 and 7.4; with and without gelatinase).

Antibacterial Activity

Minimum Inhibitory Concentration (MIC) and Minimum Bactericidal Concentration (MBC)

The MIC and MBC of IC, single nanogels, blank nanogels, and florfenicol composite nanogels against *S. aureus* 101 and SCVs 102 were determined using the broth macrodilution method. In summary, IC, single nanogels, blank nanogels, and florfenicol composite nanogels were produced in TSB at varying doses (128, 64, 32, 16, 8, 4, 2, 1, 0.5, 0.25, 1.25, 0.625, and 0.3125 μg/mL). PBS was used as a control. Conversely, 1×10^6 CFU/mL was the concentration of *S. aureus* 101 or SCVs 102. After 24 hours of culture, the MIC was eventually found to be the lowest drug concentration that significantly inhibited growth. MBC was determined by inoculating a supplemented agar plate with 100 μL of suspension with no visible bacteria from initial MIC testing. The inoculated plates were inverted and incubated at 37°C. The MBC was calculated as the concentration that lowered the viable organism count by ≥3log10 during 24 hours. Diluting the material in the agar plate by ≥250-fold decreased the drug's carryover effect. Each result was computed in triplicate.

Live/Dead Bacterial Staining Analysis

In this study, *S. aureus* 101 and SCVs 102 (1×10^6 CFU/mL) were mixed with IC, single nanogels, blank nanogels, and florfenicol composite nanogels at varied doses "0×MIC, 1/2×MIC, 1×MIC, and 2×MIC". Physiological saline was used

as a control. After a two-hour incubation period, each sample was tested with the live/dead fluorescent bacterial viability assay. A fluorescent microscope (TS2R-FL, NIKON, Japan) was used to investigate the 5 μL bacterial solution placed on a slide.

Morphological Analysis

SEM was used to investigate *S. aureus* 101 and SCVs 102 treated with IC, single nanogels, blank nanogels, florfenicol composite nanogels, and physiological saline (the control group). In summary, IC, single nanogels, blank nanogels, and florfenicol composite nanogels (all 1×MIC) were used to culture *S. aureus* 101 or SCVs 102 (1×10^6 CFU/mL) in triplicate on a cover glass for 24 hours at 37°C. Following that, the bacteria were healed and dried out. In a nutshell, the samples were fixed with 2.5% glutaraldehyde for two hours at 4°C. After cleaning the surfaces twice for 15 minutes each, the sample was dried using ethanol concentrations of 30%, 50%, 70%, 90%, 95%, and 100% for a total of 20 minutes. Finally, each sample was examined by SEM after critical point drying and gold sputter coating.

Cytotoxicity Assays

The cytotoxicity assays of IC, single nanogels, blank nanogels, and florfenicol composite nanogels in mouse fibroblast (L929 cells) were evaluated by methyl thiazolyl tetrazolium (MTT) method. Briefly, the different formulations, combined with L929 cells, were placed into a 96-well microtiter plate and incubated at 37°C for 4 h, respectively. Subsequently, the cells were stained with Alamar Blue and further incubated at 37°C for 24 and 48 hours. The fluorescence intensity was measured with a microplate reader to evaluate the cytotoxicity of the different formulations. Finally, the cell viability of IC, single nanogels, blank nanogels, and florfenicol composite nanogels were calculated.

Statistical Analysis

The experiment data are presented as Mean±S.D. and evaluated using one-way ANOVA using the SPSS 19.0 software. A *p*-value of less than 0.05 indicates statistical significance.

Result and Discussion

Optimal Formula

The standard curve of florfenicol was drawn and shown in Figure S1. The standard curve of florfenicol was y=0.001970 x+0.03495, and the linear range of the standard curves of florfenicol ranged from 25 to 1000 μg/mL (R^2=0.998) (Figure S1). On this basis, the concentration of β-CD, gelatin, γ-PGA, and TPP was used as variables, and EE and LC were used as indicators to screen their optimal formulas of florfenicol composite nanogels through box-behnken response surface (Table 1). The amount and percentage of various excipients determine the formulation's EE and LC. The higher the LC and EE, the more medicines are contained in the formulation. When LC is at its peak, the ideal number and percentage of florfenicol composite nanogels are produced.[21,22] The high drug loading and entrapment efficiency could be attributed to the drug's preferential localization within the polymer matrix, which is less hydrophilic than the external aqueous environment, given that florfenicol has been reported as a broad-spectrum antibiotic with low aqueous solubility.

The response surface approach makes it easier to investigate and model formulation obstacles and process parameters by calculating the connection between the produced response surfaces and the controlled input parameters. It accomplishes this by combining statistical and mathematical techniques.[23] Thirteen experimental runs with three repeating center points were required to provide an accurate estimate of the prediction variance throughout the whole model's design space. The experimental design and results generated by the Design-Expert program are presented in Table 1. The results of the thirty groups were displayed in Tables 2 and 3 after analysis, along with the quadratic polynomial regression equation that connected the LC to three factors:

$$LC=12.52+0.3611*A+1.65*B-1.10*C-0.9111*D-1.03*AB-1.14*AC-0.1313*AD-3.92*BC+0.2437*BD-0.7938*CD-5.43*A^2+0.8667*B^2+4.12*C^2+3.32*D^2$$

Table 2 ANOVA of LC Model

Source	Sum of Squares	df	Mean Square	F-value	P-value	
Model	542.20	14	38.73	51.57	< 0.0001	Significant
A-β-CD	2.35	1	2.35	3.13	0.0974	
B-Gelatin	49.01	1	49.01	65.25	< 0.0001	
C-γ-PGA	21.78	1	21.78	29.00	< 0.0001	
D-TPP	14.94	1	14.94	19.90	0.0005	
AB	17.02	1	17.02	22.66	0.0003	
AC	20.93	1	20.93	27.87	< 0.0001	
AD	0.2756	1	0.2756	0.3670	0.5537	
BC	245.71	1	245.71	327.17	< 0.0001	
BD	0.9506	1	0.9506	1.27	0.2782	
CD	10.08	1	10.08	13.42	0.0023	
A^2	76.49	1	76.49	101.84	< 0.0001	
B^2	1.95	1	1.95	2.59	0.1283	
C^2	43.91	1	43.91	58.47	< 0.0001	
D^2	28.50	1	28.50	37.95	< 0.0001	
Residual	11.27	15	0.7510			
Lack of Fit	11.27	10	1.13			
Pure Error	0.0000	5	0.0000			
Cor Total	553.47	29				
R^2	0.9796					
Adj-R^2	0.9606					
Pre-R^2	0.9031					
Adeq precision	25.7975					
CV%	6.09					
Mean	14.24					
Std.Dev.	0.8666					

Abbreviations: LC, loading capacity; β-CD, β-cyclodextrins; γ-PGA, γ-polyglutamic acid; TPP, sodium tripolyphosphate.

Table 3 ANOVA of EE Model

Source	Sum of Squares	df	Mean Square	F-value	P-value	
Model	382.96	14	27.35	74.16	< 0.0001	Significant
A-β-CD	52.36	1	52.36	141.96	< 0.0001	
B-Gelatin	9.10	1	9.10	24.68	0.0002	
C-γ-PGA	0.6806	1	0.6806	1.85	0.1944	
D-TPP	8.96	1	8.96	24.29	0.0002	
AB	9.46	1	9.46	25.64	0.0001	
AC	15.02	1	15.02	40.71	< 0.0001	
AD	41.93	1	41.93	113.67	< 0.0001	
BC	218.30	1	218.30	591.85	< 0.0001	
BD	17.02	1	17.02	46.13	< 0.0001	
CD	0.5256	1	0.5256	1.43	0.2511	
A^2	0.6893	1	0.6893	1.87	0.1918	
B^2	1.52	1	1.52	4.12	0.0605	
C^2	0.1206	1	0.1206	0.3271	0.5758	
D^2	0.2093	1	0.2093	0.5674	0.4630	
Residual	5.53	15	0.3688			
Lack of Fit	5.53	10	0.5533			
Pure Error	0.0000	5	0.0000			

(*Continued*)

Table 3 (Continued).

Source	Sum of Squares	df	Mean Square	F-value	P-value	
Cor Total	388.49	29				
R^2	0.9858					
Adj-R^2	0.9725					
Pre-R^2	0.9313					
Adeq precision	37.0991					
CV%	1.59					
Mean	38.28					
Std.Dev.	0.6073					

Abbreviations: EE, encapsulation efficiency; β-CD, β-cyclodextrins; γ-PGA, γ-polyglutamic acid; TPP, sodium tripolyphosphate.

The quadratic polynomial regression equation between the EE and three factors was:

$$EE=39.01+1.71*A+0.7111*B-0.1944*C-0.7056*D-0.7687*AB-0.9687*AC-1.62*AD-3.69*BC+1.03*BD+0.1813*CD-0.5158*A^2-0.7658*B^2-0.2158*C^2+0.2842*D^2$$

While the lack of fit was not significant ($p > 0.05$), the differences between the various treatments of the EE and LC models were extremely significant ($p < 0.01$). This suggests that the residuals were wholly the product of random errors. Both prediction models were shown to be dependable by the regression equation coefficient R^2 and adjusted R^2, which both show higher than 90% and reflect the range of the response values. Using the information above as a basis, three-dimensional reaction surface pictures were created (Figure 2A and B). The optimized florfenicol composite nanogels according to Design-Expert software were 73.846 mg/mL β-CD, 149.97 mg/mL gelatin, 10.0014 mg/mL γ-PGA, and 0.51425 mg/mL TPP, respectively. In this case, LC and EE of florfenicol composite nanogels were the largest, and the therapeutic effect may be the most satisfactory. The LC and EE predicted by the software were 22.8007% and 45.6005%, respectively (Figure 2C). Subsequently, the optimal formulation was verified by producing florfenicol composite nanogels with 75 mg/mL β-CD, 150 mg/mL gelatin, 10 mg/mL γ-PGA, and 0.5 mg/mL TPP, respectively. The LC and EE of prepared florfenicol composite nanogels were 23.5%±4.6% and 45.3%±2.7%, respectively. Thus, the optimal preparation method for the florfenicol composite nanogels designed by the Box-Behnken response surface technique was accurate and reliable.

Optimal Formula

Characterization

In this study, florfenicol was encapsulated into β-CD to form florfenicol IC that was got through complexation to improve the sustained release effect. On the other hand, the γ-PGA-gelatin nanogels loaded with florfenicol were obtained through the electrostatic interaction between gelatin (with a positive charge) and γ-PGA (with a negative charge) with the help of TPP (ionic crosslinking agent) to improve the targeted release effect. Finally, florfenicol composite nanogels were prepared by self-assembly with sustained and targeted release effects (Figure 3A).

Subsequently, the appearance, TEM, SEM, EDS, size, ZP, UV-vis spectrophotometry, FTIR spectrum, and PXRD of IC, single nanogels, blank nanogels, and florfenicol composite nanogels were shown in Figure 3B–J and Figures S2–S7. The appearance of IC in the bottle was a clear transparent color and showed the characteristic of flowing like water at 0°, 45°, 90°, and 180° (Figure S2); Interestingly, the appearance of single nanogels, blank nanogels, florfenicol composite nanogels in the bottle were all faint yellow and showed excellent gel properties at 0°, 45°, 90°, and 180° (Figures 3B and S2). Meanwhile, TEM showed that IC, single nanogels, blank nanogels, and florfenicol composite nanogels were spherical with a smooth surface and good particle size distributions (Figures 3C and S3). This suggests that the aforementioned materials were successfully prepared. Additionally, the freeze-dried IC, single nanogels, blank nanogels, and florfenicol composite nanogels showed a three-dimensional network structure, which were highly beneficial for the transportation of drugs, oxygen, and

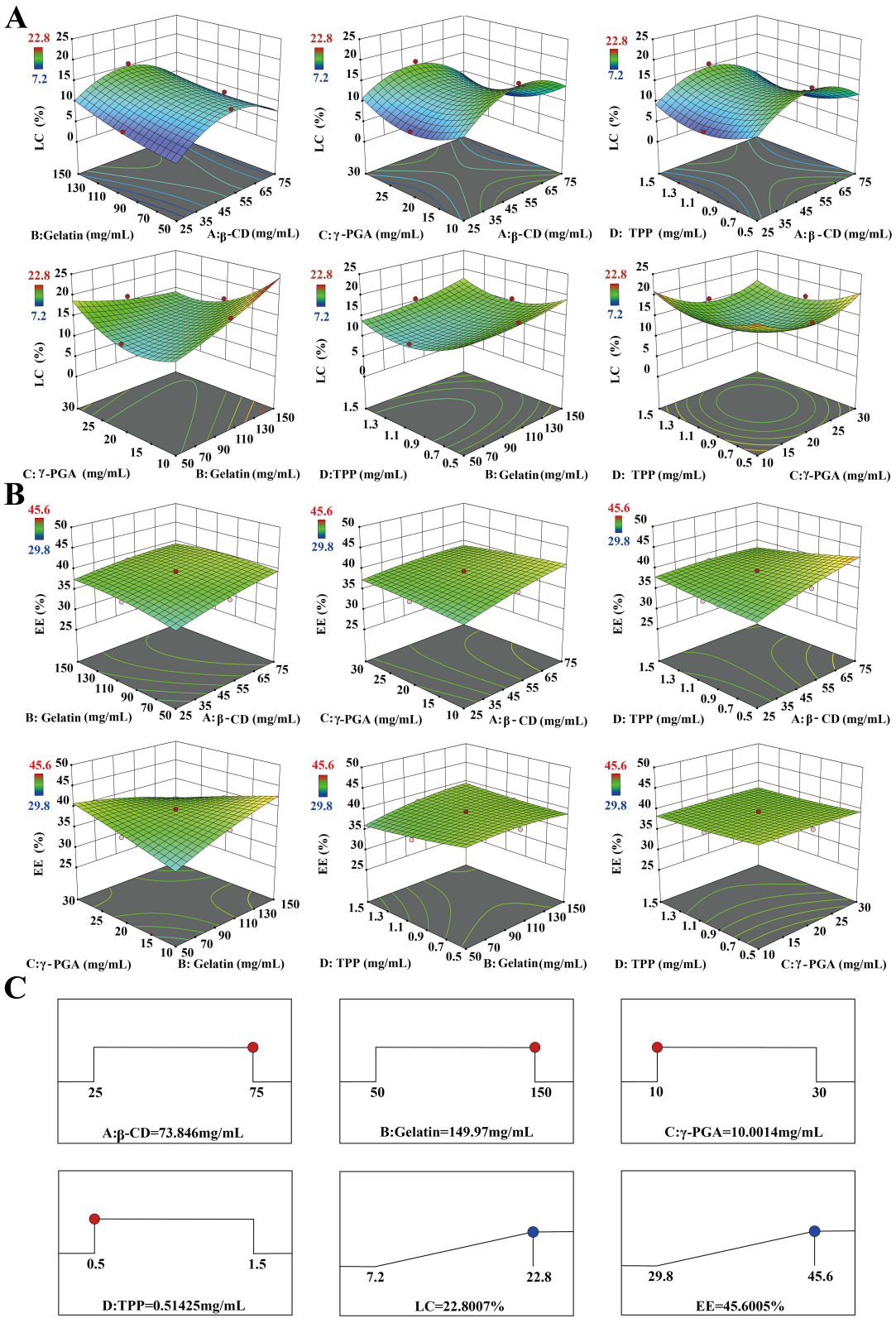

Figure 2 Screening of the optimal formulation of florfenicol composite nanogels. Three-dimensional arrangement for response surface images of the different concentrations of β-CD, gelatin, γ-PGA, and TPP to LC (**A**) and EE (**B**). (**C**) The optimal formula predicted by Design-Expert software.

https://doi.org/10.2147/IJN.S511947

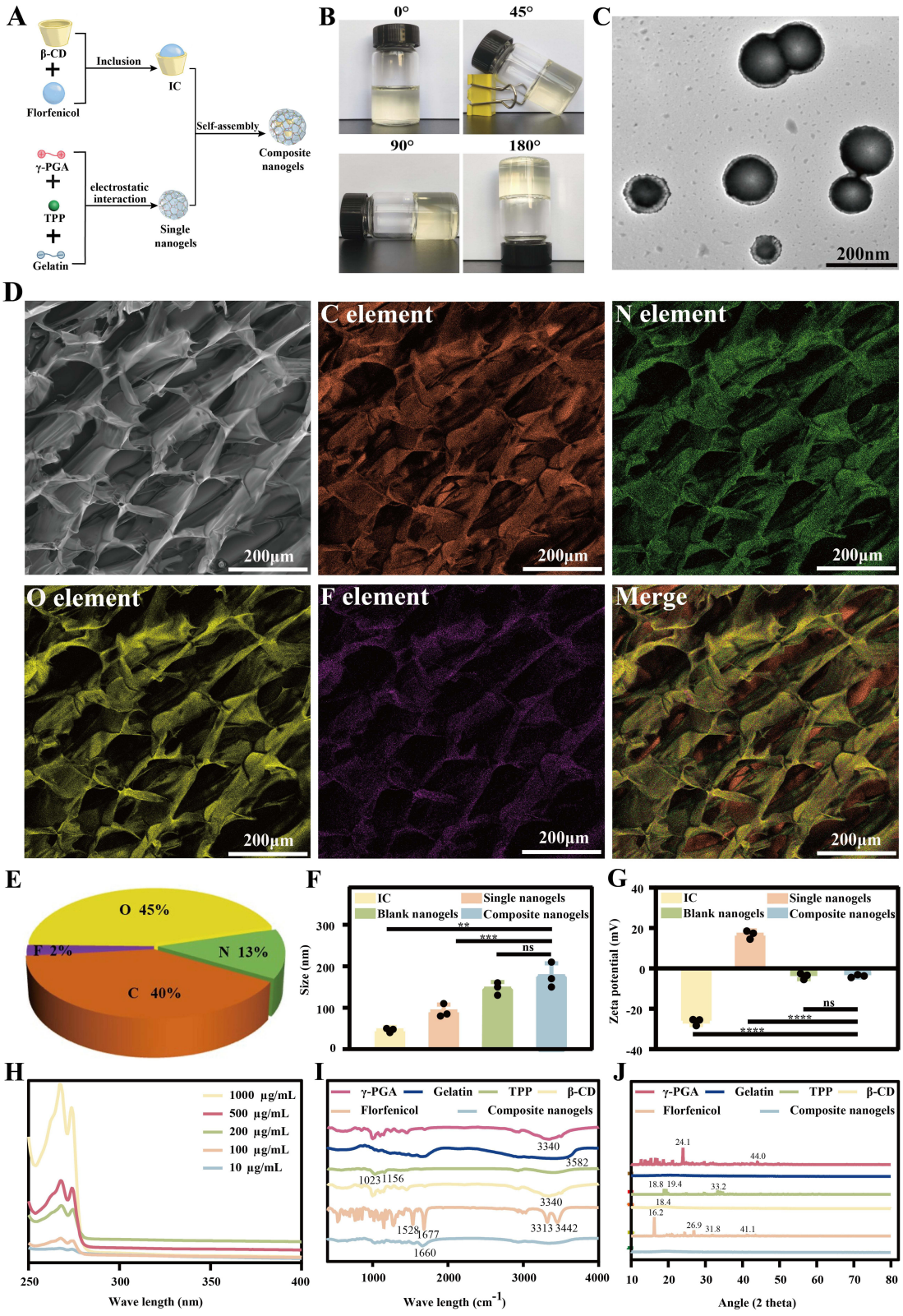

Figure 3 Characterization of florfenicol composite nanogels. (**A**) Schematic illustration of the preparation process of florfenicol composite nanogels; (**B**) Appearance in a bottle (0°, 45°, 90°, and 180°); (**C**) TEM; (**D**) SEM and EDS; (**E**) Percentage of element (C, N, O and F); (**F**) Size distribution; (**G**) Zeta potential; (**H**) UV-vis absorption spectra; (**I**) FTIR; (**J**) XRD (**P < 0.01, ***P< 0.001, and ****P< 0.001).

nutrients, as well as the absorption of exudate at the bacterial inflammatory site (Figures 3D and S4). Furthermore, the EDS of florfenicol composite nanogels indicated that C, N, O, and F were uniformly distributed in the florfenicol composite nanogels. Thus, florfenicol was evenly distributed in the florfenicol composite nanogels, which also proved that the florfenicol composite nanogels were successfully prepared. In florfenicol composite nanogels, the percentage of C, N, O, and F elements was 40%, 13%, 45%, and 2%, respectively (Figure 3E).

The mean size of IC, single nanogels, blank nanogels, and florfenicol composite nanogels were 46.0±4.3 nm, 91.7 ±13.1 nm, 146.7±12.5 nm, and 176.7±24.9 nm, respectively (Figure 3F). The particle size gradually increases, which also indicates that florfenicol is encapsulated by biomaterial (β-CD, gelatin, γ-PGA, and TPP). The ZP of IC, single nanogels, blank nanogels, and florfenicol composite nanogels were −26.4±1.3 mV, 16.8±1.7 mV, −3.8±1.2 mV, and −3.7±0.6 mV, respectively (Figure 3G). Due to the negative ZP exhibited by β-CD, IC was also displayed as having a negative ZP (−26.4±1.3 mV). Subsequently, single nanogels were shown to be positive ZP (16.8±1.7 mV) due to gelatin being positive. Blank nanogels and florfenicol composite nanogels were both negative ZP (−3.8±1.2 mV and −3.7±0.6 mV), which may be caused by the addition of β-CD. The changes in size and ZP also indicated that IC, single nanogels, blank nanogels, and florfenicol composite nanogels were successfully prepared.

The UV-vis absorption spectra showed that the characteristic absorption peaks of IC contained λ_{max}=259 nm, single nanogels contained λ_{max}=268 nm and λ_{max}=273 nm, blank nanogels contained λ_{max}=λ_{max}=266 nm and λ_{max}=275 nm, and florfenicol composite nanogels contained λ_{max}=266 nm and λ_{max}=275 nm (Figures 3H and S5). When the concentration of florfenicol composite nanogels was 10 μg/mL, these two characteristic absorption peaks were difficult to observe. However, when the concentration was 100 μg/mL, these two characteristic absorption peaks were clearly observed, and as the concentration increased, these two peaks became more obvious. The FTIR spectrum of γ-PGA, gelatin, TPP, β-CD, florfenicol, IC, single nanogels, blank nanogels, and florfenicol composite nanogels were shown in Figures 3I and S6. FTIR spectroscopy was used to study drug-hydrogel interactions. Interestingly, the FTIR spectroscopy of β-CD and IC were similar, and the FTIR spectroscopy of blank nanogels and florfenicol composite nanogels were similar. The new characteristic peaks (1653 and 3420 cm^{-1}) of single nanogels were shown. The distinctive peaks for γ-PGA at 3340 cm^{-1}, gelatin at 3582 cm^{-1}, TPP at 1023 and 1156 cm^{-1}, β-CD at 3340 cm^{-1}, and florfenicol at 1528, 1667, 3313, and 3442 cm^{-1} vanished from the spectrum of florfenicol composite nanogels, and new characteristic peaks (1660 cm^{-1}) were visible instead, which may be attributed to the complexation of β-CD and electrostatic interaction between gelatin (positive charge) and γ-PGA (negative charge) using TPP (ionic crosslinkers). Thus, the preparation of the florfenicol composite nanogels was successful. XRD was used to determine the crystallinity and physical state of γ-PGA, gelatin, TPP, β-CD, florfenicol, IC, single nanogels, blank nanogels, and florfenicol composite nanogels. The characteristic diffraction peaks of γ-PGA (24.1◦ and 44.0◦), TPP (18.8◦, 19.4◦, and 33.2◦), TPP (18.8◦, 19.4◦, and 33.2◦), β-CD (18.4◦), and florfenicol (16.2◦, 26.9◦, 31.8 ◦, and 41.1◦) were shown in Figures 3J and S7. It was worth noting that the characteristic diffraction peaks of florfenicol had almost disappeared in florfenicol composite nanogels due to the formation of florfenicol IC-loaded γ-PGA@gelatin composite nanogels. The unique diffraction peaks of the florfenicol composite nanogels vanished, and this is likely due to complexation and electrostatic interaction.

pH/Gelatinase-Double Responsiveness

Considering the pH-responsiveness of γ-PGA and the gelatinase-responsiveness of gelatin, the prepared florfenicol composite nanogels may have pH/gelatinase dual responsiveness. Thus, lyophilized single nanogels, blank nanogels, and florfenicol composite nanogels were put in different microenvironments (pH 7.4 without gelatinase; pH 5.5 without gelatinase; pH 7.4 with gelatinase; and pH 5.5 with gelatinase), and the morphology was observed at 0, 0.5, 1, 2, 3, 4, 6, 8, 12, and 24 h, respectively. The lyophilized single nanogels were destroyed at pH 7.4 without gelatinase at 12 h, at pH 5.5 without gelatinase at 6 h, on the other hand, it was destroyed at pH 7.4 with gelatinase and pH 5.5 with gelatinase at 3 h (Figure S8). At 24 h, the lyophilized blank nanogels still have a complete morphology at pH 7.4 without gelatinase, but significant swelling occurs at pH 5.5 without gelatinase. Meanwhile, the lyophilized blank nanogels were completely destroyed at pH 7.4 with gelatinase at 6 h, but it was completely destroyed at pH 5.5 with gelatinase at 2 h (Figure S9). At pH 7.4 without gelatinase, the morphology of lyophilized single nanogels, blank nanogels, and florfenicol composite nanogels had no obvious change. Interestingly, the appearance of lyophilized single nanogels, blank nanogels, and

florfenicol composite nanogels had changed significantly at pH 5.5 without gelatinase and at pH 7.4 with gelatinase. Furthermore, the morphology of lyophilized single nanogels, blank nanogels, and florfenicol composite nanogels were severely damaged at pH 5.5 with gelatinase (Figure 4A).

Considering the microenvironment (pH 5.5 and gelatinase) of bacterial dairy cows' mastitis, the release of the florfenicol composite nanogels in PBS (pH 5.5/7.4) with and without gelatinase at 37±0.5°C was estimated to determine the environmental pH/gelatinase dual responsiveness. After 24 hours, 54.6%±5.4% (Figure 4B) of the florfenicol was released at pH 7.4 in the absence of gelatinase, whereas 97.3%±1.9% (Figure 4D) of the drug was released at pH 7.4 in

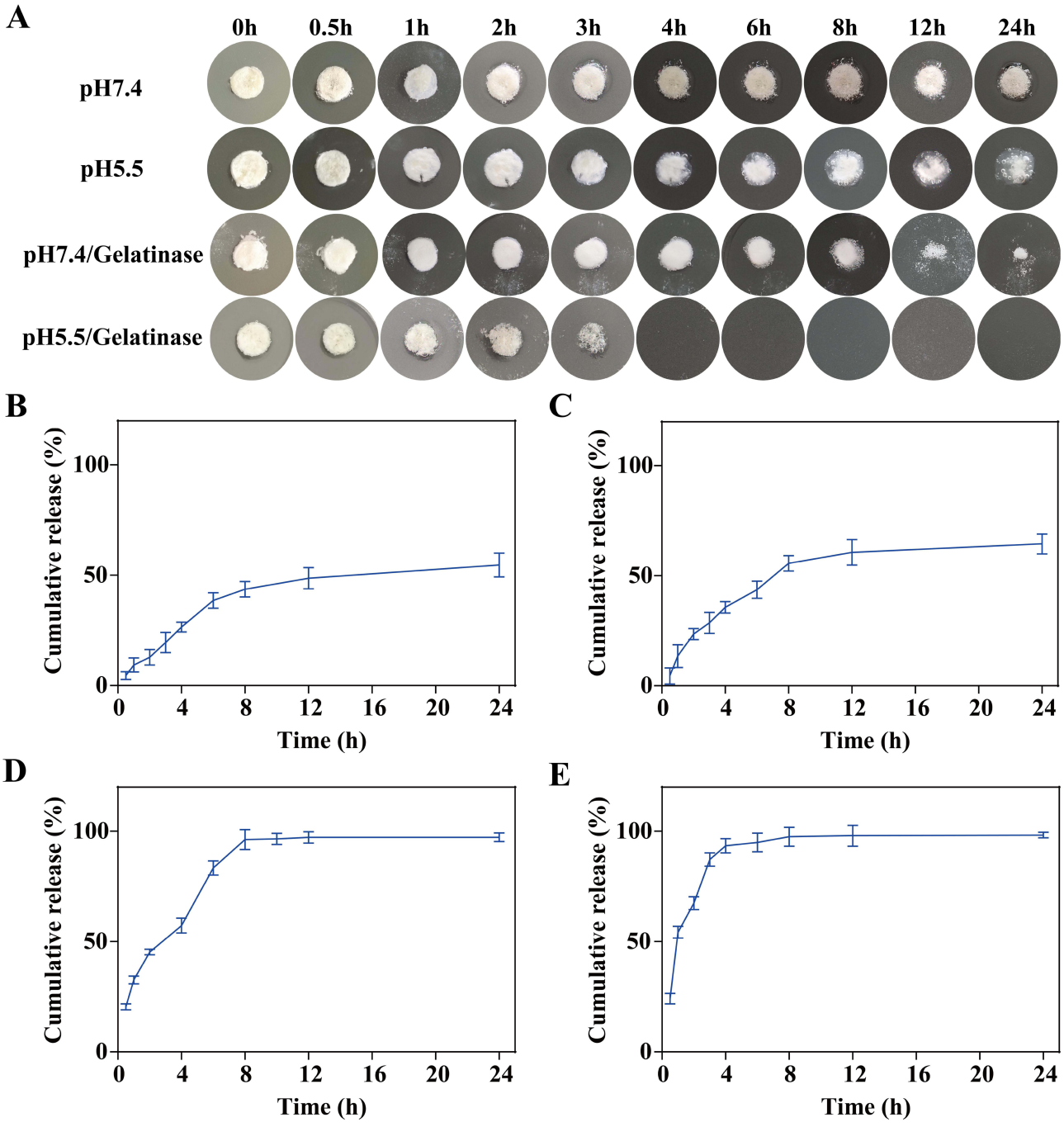

Figure 4 Improving targeted release of florfenicol composite nanogels through pH/gelatinase dual responsiveness. (**A**) Morphology change of florfenicol composite nanogels in different microenvironments; In vitro release of florfenicol composite nanogels in different microenvironments ((**B**) pH 7.4 without gelatinase; (**C**) pH 5.5 without gelatinase; (**D**) pH 7.4 with gelatinase; (**E**) pH 5.5 with gelatinase).

the presence of gelatinase. Additionally, at pH 5.5 without gelatinase, 64.5%± 4.6% (Figure 4C) of the florfenicol was released, whereas at pH 5.5 with gelatinase, 98.3%±1.2% (Figure 4E) was released. These findings indicated that the prepared florfenicol composite nanogels displayed pH/gelatinase dual responsiveness and on-demand release performance due to the pH-responsiveness of γ-PGA and the gelatinase-responsiveness of gelatin. This might be because strongly protonated amino groups in pH 5.5 repel one another, creating holes that let water molecules enter and grow into the nanogels' cores. At the same time, gelatin in the role of gelatinase and the florfenicol composite nanogels had been split. On the contrary, at higher pH values (pH 7.4), florfenicol composite nanogels with low protonation result in a smaller swelling rate. Thus, the swelling rate of florfenicol composite nanogels was higher under the action of gelatinase and pH 5.5. This may be attributed to the splitting and swelling of florfenicol composite nanogels acted by gelatinase and pH 5.5, which allows a large number of water molecules to enter the florfenicol composite nanogels for swelling. Thus, florfenicol composite nanogels exhibited obvious pH/gelatinase-double responsiveness.

Antibacterial Activity

The antibacterial activity of IC, single nanogels, blank nanogels, and florfenicol composite nanogels against *S. aureus* 101 and SCVs 102 was shown in Table 4 and Figure 5. The MIC of IC, single nanogels, blank nanogels, and florfenicol composite nanogels were 4, 2, >128, and 2 μg/mL for *S. aureus* 101 and 4, 2, >128, and 1 μg/mL for SCVs 102, respectively. The MBC of IC, single nanogels, blank nanogels, and florfenicol composite nanogels were 16, 16, >128, and 8 μg/mL for *S. aureus* 101 and 8, 4, >128, and 2 μg/mL for SCVs 102, respectively (Table 4). Thus, as compared to IC, single nanogels, blank nanogels, and florfenicol composite nanogels showed higher antibacterial activity against *S. aureus* 101 and SCVs 102. The enhanced antibacterial activity may be due to the sustained and targeted release effects of florfenicol composite nanogels. Florfenicol was released in a sustained and intelligent manner within the three-dimensional network structure, thanks to the complexation of β-CD and the double responsiveness of gelatinase and pH. This prolonged the drug's action period and raised its concentration at the site of bacterial infection. Meanwhile, the inhibition zones of IC, single nanogels, blank nanogels, and florfenicol composite nanogels were 1.97±0.13, 2.23±0.12, 0.37±0.11, and 2.63±0.12 cm for *S. aureus* 101 (Figure 5A) and 2.07±0.17, 2.53±0.05, 0.77±0.05, and 2.83±0.05 cm for SCVs 102, respectively (Figure 5B). Therefore, compared with IC, single nanogels, blank nanogels, and florfenicol composite nanogels had larger inhibition zones, which means that florfenicol composite nanogels had stronger antibacterial activity.

Furthermore, the mixture of *S. aureus* 101 or SCVs 102 and florfenicol composite nanogels (0×MIC, 1/2×MIC, 1×MIC, and 2×MIC) was treated using the live/dead bacterial staining kit. With the increase of florfenicol composite nanogels drug concentration, it can be proved that the number of live bacterial cells (red) increases and the number of dead bacterial cells (green) decreases (Figure 5C). The findings from the inhibition zones and MICs were consistent with these results. Interestingly, florfenicol composite nanogels had stronger antibacterial activity against SCVs 102 than *S. aureus* 101. This may be because the cell membranes of SCVs 102 were more easily damaged by florfenicol composite nanogels. To verify this hypothesis, SEM was used to observe *S. aureus* 101 or SCVs 102 treated with IC, single nanogels, blank nanogels, and florfenicol composite nanogels, as well as physiological saline (the control group). Compared with the control group, blank nanogels had no significant effect against *S. aureus* 101 and SCVs 102.

Table 4 MIC and MBC (μg/mL)

	MIC		MBC	
	101 strains	102 strains	101 strains	102 strains
IC	4	4	16	8
Single nanogels	2	2	16	4
Blank nanogels	>128	>128	>128	>128
Composite nanogels	2	1	8	2

Abbreviations: MIC, minimum inhibitory concentration; MBC, minimum bactericidal concentration; IC, inclusion complex.

https://doi.org/10.2147/IJN.S511947

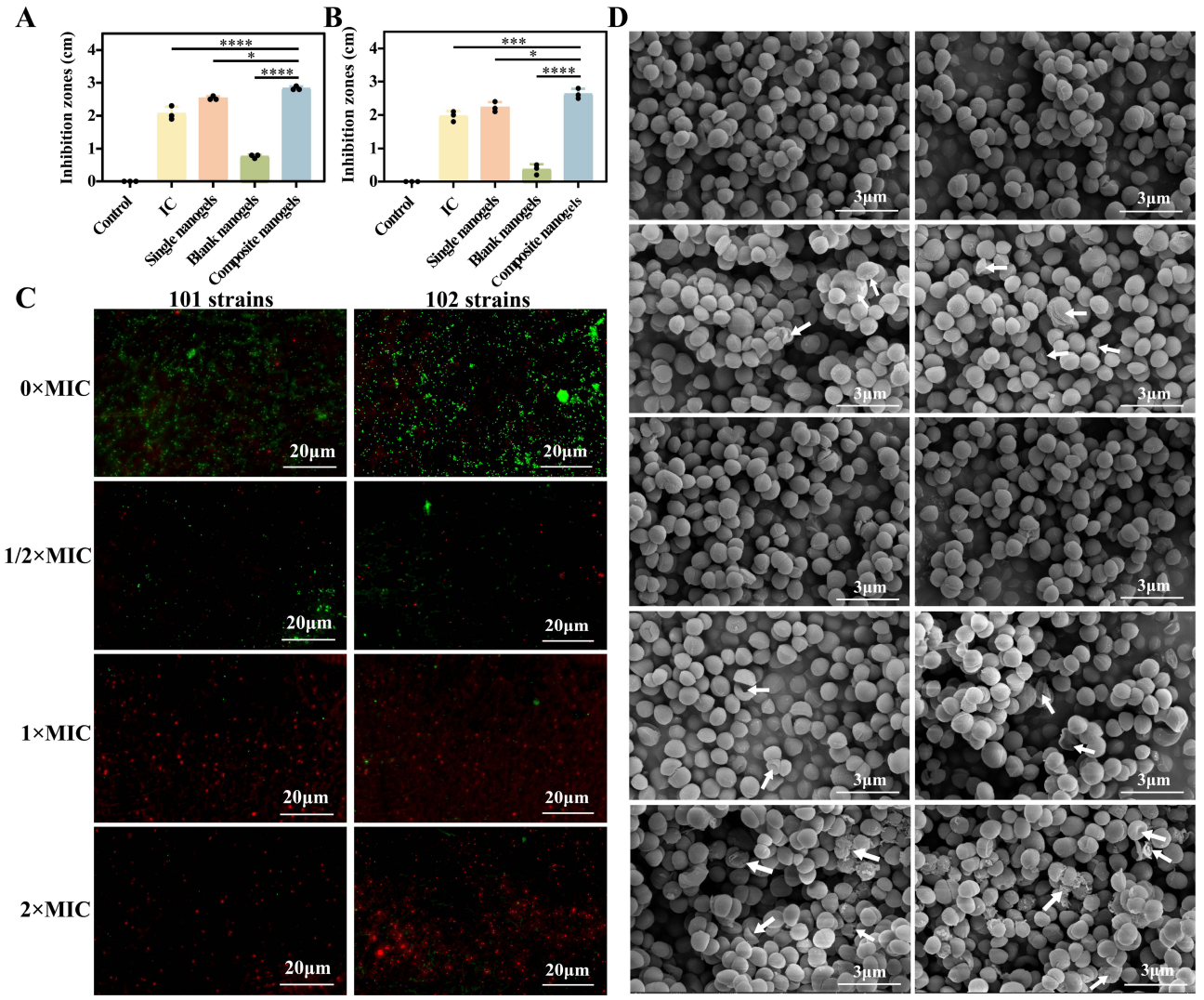

Figure 5 The antibacterial effect of IC, single nanogels, blank nanogels and florfenicol composite nanogels against *S. aureus* 101 strains and SCVs 102 strains. (**A**) inhibition zones (*S. aureus* 101 strains); (**B**) inhibition zones (SCVs 102 strains); (**C**) live/dead bacterial staining; (**D**) SEM image (*$P < 0.05$, **$P < 0.01$, ***$P < 0.001$, and ****$P < 0.001$).

However, after the action of IC, single nanogels, blank nanogels, and florfenicol composite nanogels had significant effects against *S. aureus* 101 and SCVs 102, the holes appeared due to damage to the bacterial cell membrane and cell wall. In particular, the holes in the florfenicol composite nanogels group were more obvious. At the same time, the bacteria also underwent severe rupture and indentation, and the contents flowed out from the bacteria, which may indicate that the florfenicol composite nanogels have damaged the cell membrane and cell wall of the bacteria (Figure 5D). In addition, as a new drug delivery system, the prepared florfenicol composite nanogels may also show significant potential in the treatment of human device infections caused by SCVs, such as prosthetic joint infections. This may be because the nanogels can enhance the affinity between the drug and the infection site, further promote the local drug release, and inhibit the growth of bacteria.[24]

Cytotoxicity Evaluation

Through cytotoxicity test, the safety of different formulations of targeted cells (L929 cells) was truly evaluated by taking the growth of L929 cells as an indicator. This helps to determine the safety of drug delivery systems for in vivo applications, avoiding cell damage or toxicity. After 48 h of cultivation, the L929 cells in IC, single nanogels, blank nanogels, and florfenicol composite nanogels group exhibited healthy growth and proliferation compared with the control

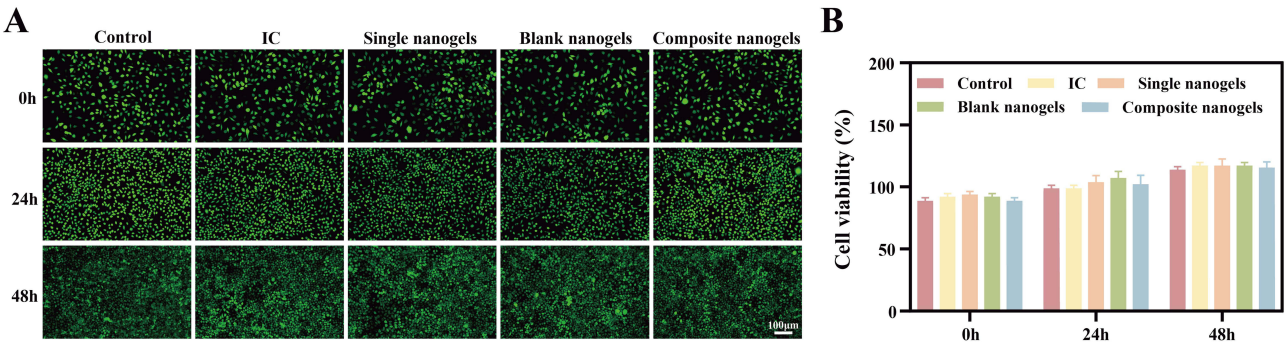

Figure 6 In vitro biosafety studies. (**A**) cell cultured with nanogels dressing after 24h; (**B**) cell viability.

group (Figure 6A). Simultaneously, the viability of the L929 cells incubated with IC, single nanogels, blank nanogels, and florfenicol composite nanogels for 24 h was maintained above 95% (Figure 6B). Thus, these results indicated the excellent cytocompatibility of the florfenicol composite nanogels.

Conclusions

S. aureus commonly endures in the body as SCVs, avoiding the bactericidal effects of drugs and leading to persistent and recurring mastitis infections in cows. Nevertheless, florfenicol is widely dispersed throughout the body and is challenging to penetrate to the targeted site at an appropriate therapeutic dosage, florfenicol's effectiveness in treating dairy cow mastitis caused by SCVs is comparatively low. Thus, florfenicol may be encapsulated into β-CD to obtain florfenicol IC through complexation, thereby improving the sustained release effect. Then, with the help of TPP (ionic crosslinking agent), the γ-PGA-gelatin nanogels were prepared through the electrostatic interaction between gelatin (with positive charge) and γ-PGA (with negative charge), thereby improving the targeted release effect (the double responsiveness of gelatinase and pH). In this work, florfenicol composite nanogels with sustained and targeted release effects were successfully prepared by complexation and electrostatic interaction and further evaluated by physicochemical characterization. Furthermore, its pH/gelatinase-double responsiveness and enhanced antibacterial effects were confirmed. In conclusion, we confirmed our hypothesis that florfenicol composite nanogels with sustained and targeted release effects can boost the antibacterial activity of florfenicol against SCVs.

Data Sharing Statement

The data used to support the findings of this study are available from the corresponding author upon request.

Acknowledgments

The article was supported financially by the Natural Science Support Program of Xinjiang Production and Construction Corps (2024DA029), the second group of the Tianshan Talent Training Program: Youth Support Talent Project (2023TSYCQNTJ0033), and the National Natural Science Foundation of China (32460904). The authors thank Sun beibei, Ma guocai, and Wang Lijun from the Instrumental Analysis Center, at Tarim University for their support of the instrument (SEM, TEM, and Laser confocal microscope). The authors would like to thank Wang Wenqian from Shiyanjia Lab (www.shiyanjia.com) for the FTIR analysis.

Disclosure

The authors declare no conflicts of interest in this work.

References

1. Alves JS, de Moura Souza R, Lima Moreira JP, Gonzalez AGM. Antimicrobial resistance of *Enterobacteriaceae* and *Staphylococcus* spp. isolated from raw cow's milk from healthy, clinical and subclinical mastitis udders. *Preventive Vet Med*. 2024;227:106205. doi:10.1016/j.prevetmed.2024.106205

2. Obermueller M, Traby L, Weiss-Tessbach M, et al. *Staphylococcus aureus* small colony variants: a potentially underestimated microbiological challenge in peritoneal dialysis. *Int J Antimicrob Agents*. 2024;63(5):107135. doi:10.1016/j.ijantimicag.2024.107135
3. Staudacher M, Hotz JF, Kriz R, et al. Differences in oxazolidinone resistance mechanisms and small colony variants emergence of *Staphylococcus aureus* induced in an *in vitro* resistance development model. *Emerging Microbes Infect*. 2024;13(1):2292077. doi:10.1080/22221751.2023.2292077
4. Luo W, Liu J, Zhang M, et al. Florfenicol core-shell composite nanogels as oral administration for efficient treatment of bacterial enteritis. *Int J Pharm*. 2024;662:124499. doi:10.1016/j.ijpharm.2024.124499
5. Brenciani A, Coccitto SN, Cucco L, et al. Emerging resistance to florfenicol in actinobacillus pleuropneumoniae isolates on two Italian pig farms. *Vet Microbiol*. 2024;296:110186. doi:10.1016/j.vetmic.2024.110186
6. Gharbi M, Tiss R, Hamdi C, Hamrouni S, Maaroufi A. Occurrence of florfenicol and linezolid resistance and emergence of *optrA* gene in *Campylobacter coli* isolates from tunisian avian farms. *Int J Microbiol*. 2024;2024:1694745. doi:10.1155/2024/1694745
7. Liu J, Ju M, Wu Y, Leng N, Algharib SA, Luo W. Antibacterial activity of florfenicol composite nanogels against *Staphylococcus aureus* small colony variants. *J Veterin Sci*. 2022;23(5):e78. doi:10.4142/jvs.22046
8. Yang Z, Huang R, Zheng B, et al. Highly stretchable, adhesive, biocompatible, and antibacterial hydrogel dressings for wound healing. *Adv Sci*. 2021;8(8):2003627. doi:10.1002/advs.202003627
9. Liu Y, Chen D, Zhang A, et al. Composite inclusion complexes containing hyaluronic acid/chitosan nanosystems for dual responsive enrofloxacin release. *Carbohydr Polym*. 2021;252:117162. doi:10.1016/j.carbpol.2020.117162
10. Shu QH, Zuo RT, Chu M, et al. Fiber-reinforced gelatin/β-cyclodextrin hydrogels loaded with platelet-rich plasma-derived exosomes for diabetic wound healing. *Biomat Adv*. 2023;154:213640. doi:10.1016/j.bioadv.2023.213640
11. Luo W, Zhang M, Jiang Y, et al. Manipulated slow release of florfenicol hydrogels for effective treatment of anti-intestinal bacterial infections. *Int j Nanomed*. 2025;20:541–555. doi:10.2147/IJN.S484536
12. Youssef F, Mohamed G, Ismail S, Elzorba H, Elbanna H. Synthesis, characterization and in vitro antimicrobial activity of florfenicol-chitosan nanocomposite. *Egypt J Chem*. 2021;64:941–948.
13. Abonashey SG, Hassan HAFM, Shalaby MA, Fouad AG, Mobarez E, El-Banna HA. Formulation, pharmacokinetics, and antibacterial activity of florfenicol-loaded niosome. *Drug Delivery Transl Res*. 2024;14(4):1077–1092. doi:10.1007/s13346-023-01459-9
14. Mottola S, De Marco I. Supercritical antisolvent precipitation of corticosteroids/β-cyclodextrin inclusion complexes. *Polymers*. 2023;16(1):29. doi:10.3390/polym16010029
15. He Y, Zheng Y, Liu C, Zhang H, Shen J. Citric acid cross-linked β-cyclodextrins: a review of preparation and environmental/biomedical application. *Carbohydr Polym*. 2024;323:121438. doi:10.1016/j.carbpol.2023.121438
16. He D, Liao C, Li P, Liao X, Zhang S. Multifunctional photothermally responsive hydrogel as an effective whole-process management platform to accelerate chronic diabetic wound healing. *Acta Biomater*. 2024;174:153–162. doi:10.1016/j.actbio.2023.11.043
17. Li X, Liu J, Dou J, et al. Enhanced cellular delivery of tildipirosin by xanthan gum-gelatin composite nanogels. *Langmuir*. 2024;40(9):4860–4870. doi:10.1021/acs.langmuir.3c03559
18. Liu Z, He Y, Ma X. Preparation, characterization and drug delivery research of γ-polyglutamic acid nanoparticles: a review. *Curr Drug Del*. 2024;21(6):795–806. doi:10.2174/1567201820666230102140450
19. Alkasir R, Liu X, Zahra M, Ferreri M, Su J, Han B. Characteristics of *Staphylococcus aureus* small colony variant and its parent strain isolated from chronic mastitis at a dairy farm in Beijing, China. *Microb Drug Resist*. 2013;19(2):138–145. doi:10.1089/mdr.2012.0086
20. Liu J, Ju M, Guan D, Song W, Algharib SA, Luo W. Composite inclusion complexes containing sodium alginate composite nanogels for pH-responsive valnemulin hydrochloride release. *J mol Struct*. 2022;1263:133054. doi:10.1016/j.molstruc.2022.133054
21. Alian M, Saadat S, Rezaeitavabe F. An investigation on the dose-dependent effect of iron shaving on bio-hydrogen production from food waste. *Int J Hydrogen Energy*. 2021;46(38):19886–19896. doi:10.1016/j.ijhydene.2021.03.121
22. Rahimian Z, Sadrian S, Shahisavandi M, et al. Antiseizure effects of *Peganum harmala* L. and *Lavandula angustifolia*. *Biomed Res Int*. 2023;2023:4121998. doi:10.1155/2023/4121998
23. Asfour MH, Kassem AA, Salama A. Topical nanostructured lipid carriers/inorganic sunscreen combination for alleviation of all-trans retinoic acid-induced photosensitivity: box-Behnken design optimization, in vitro and in vivo evaluation. *Eur J Pharm Sci*. 2019;134:219–232. doi:10.1016/j.ejps.2019.04.019
24. Ali AA, Al Bostami RD, Al-Othman A. Nanogel-based composites for bacterial antibiofilm activity: advances, challenges, and prospects. *RSC Adv*. 2024;14(15):10546–10559. doi:10.1039/D4RA00410H